

Cite this: *Chem. Commun.*, 2011, **47**, 7446–7448

www.rsc.org/chemcomm

COMMUNICATION

Size-modulated catalytic activity of enzyme–nanoparticle conjugates: a combined kinetic and theoretical study†

Chung-Shu Wu,^a Cheng-Che Lee,^a Chia-Tien Wu,^a Yuh-Shyong Yang^b and Fu-Hsiang Ko^{*a}

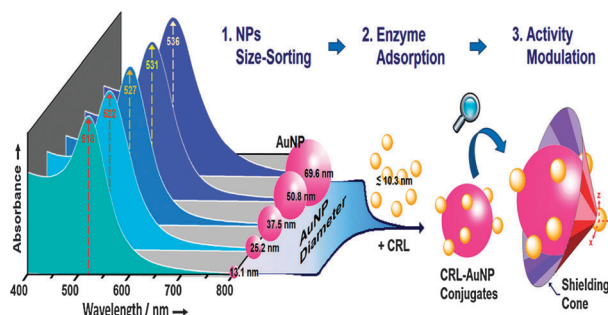
Received 22nd February 2011, Accepted 4th May 2011

DOI: 10.1039/c1cc11020a

A series of experiments were performed to systematically analyze the effect of nanoparticle (NP) size on the catalytic behavior of enzyme–NP conjugates, and a shielding model based on diffusion–collision theory was developed to explain the correlation between the size effects and the kinetic responses.

Many biomolecules, such as membrane proteins, perform their specific biorecognition or biocatalytic events while immobilized on the surfaces of cells or organelles.¹ Several artificial technologies (*e.g.*, bioconversion, bioremediation, biosensing) also take advantage of immobilized biomolecules and bio-species.² In this regard, the modification and immobilization of enzymes has been studied widely for the generation of biocatalysts exhibiting enhanced stability and selectivity.³ Several synthetic scaffolds and supports, including gels,⁴ macromolecules,⁵ planar surfaces,⁶ and nanocomposites,⁷ have been used to immobilize enzymes. Among them, nanoparticles (NPs) provide an almost ideal mix of properties—minimum diffusional limitation, maximum surface area and high effective enzyme loading—to optimize the performance of immobilized enzymes^{3,8} while harnessing the fluorescent, magnetic and interfacial behavior of the resulting nano-materials.^{7,9} However, studies of the effects of NPs size, shape and material properties on both the kinetic experiments and theoretical model of the catalytic reactions of its enzyme–NP conjugates still remain rare.

In a previous paper,¹⁰ we demonstrated that adsorbing lipase onto gold NPs (AuNPs) significantly increased its enzymatic activity. In further investigations, we observed that the size of the NPs affected the catalytic activity; based on a diffusion–collision theory, we have attempted to develop a length-scale-dependent model to explain the effect of NP size on the modulation in the activity of the enzyme–AuNP conjugate systems. In Nature, controllable modulation of enzyme activity is a potent means of regulating several cellular processes (*e.g.*, signal transduction, biosynthesis, metabolism).¹¹ The modulation of



Scheme 1 Schematic representation of the preparation of CRL–AuNP conjugates that modulate the activity of the enzyme, and a cartoon of the shielding model.

biocatalytic behavior is an attractive feature for exploitation in the field of nano-biotechnology.¹² For extended studies of biocatalysis, lipases are very suitable esterases because of their well-defined structures, properties, and applications. Lipases are used industrially in detergents, in paper and food technology, in the preparation of specialty fats, in various clinical studies, and for drug delivery.¹³ Therefore, in this study we selected *Candida rugosa* lipase (CRL, E.C. 3.1.1.3) to construct our enzyme–NP conjugates. As illustrated schematically in Scheme 1, we reported a series of experiments and a theoretical model designed to analyze the effect of AuNP size on the modulation of enzyme activity.

We selected AuNPs as the adsorption materials for CRL in this study because they can be synthesized in a variety of diameters (13–100 nm) and readily characterized using UV-Vis spectrophotometry and scanning electron microscopy (SEM). In these experiments, we used a standard chemical reduction method to prepare spherical AuNPs having mean diameters of 13.1, 25.2, 37.5, 50.8, and 69.6 nm, under conditions that ensured their stability and lack of aggregation (see ESI I†). For the preparation of enzyme-functionalized AuNPs with their colloidal stability, we performed the salt-induced colloidal tests to analyze the enzyme coverage and concentration of the protection factor (C_p ; see ESI II†), determined by measuring the ratios of the absorbance at 620 nm (A_{620}) to those of the absorption signals (A_{peak}) of the differently sized AuNPs; Fig. S5 (ESI†) displays these progress plots. To analyze the enzyme coverage, we define R as the ratio A_{peak}/A_{620} . When the enzyme concentration was sufficient to cap the AuNPs

^a Institute of Nanotechnology, and Department of Materials Science and Engineering, National Chiao Tung University, Hsinchu 300, Taiwan. E-mail: fhko@mail.nctu.edu.tw

^b Department of Biological Science and Technology, National Chiao Tung University, Hsinchu 300, Taiwan

† Electronic supplementary information (ESI) available: Experimental details, theoretical considerations and additional analyses. See DOI: 10.1039/c1cc11020a

Table 1 Experiment-measured and theoretical kinetic constants for the CRL–AuNP conjugates and planar surface-immobilized CRL systems

AuNP size/nm	$k_{\text{cat}}/\text{s}^{-1}$	$K_{\text{m}}/\mu\text{M}$	$k_{\text{cat}}/K_{\text{m}}/\mu\text{M}^{-1}\text{s}^{-1}$	μ/cP	$k_{\text{max}}^{\text{eff}}/\mu\text{M}^{-1}\text{s}^{-1}$	η	$\exp(-E_{\text{act}}/RT)$ at 303 K	$k_{\text{E-NP}}^{\text{coll}}/\mu\text{M}^{-1}\text{s}^{-1}$
NP size $\rightarrow 0$	—	—	—	$(1.13 \pm 0.017)^b$	15.56	1.00		1.37
13.1	18.0 ± 0.56	9.5 ± 1.02	1.89 ± 0.26	1.14 ± 0.016	15.11	0.91		1.22
25.2	18.3 ± 0.26	14.1 ± 0.68	1.30 ± 0.08	1.14 ± 0.012	14.97	0.85		1.12
37.5	19.6 ± 0.43	15.7 ± 1.11	1.25 ± 0.12	1.14 ± 0.016	14.90	0.81		1.06
50.8	19.1 ± 0.30	17.1 ± 0.84	1.12 ± 0.07	1.12 ± 0.016	15.11	0.78	0.0880 ± 0.0058	1.03
69.6	17.9 ± 0.38	18.1 ± 1.20	0.99 ± 0.09	1.13 ± 0.025	14.92	0.75		0.98
Immobilized on a planar surface (NP size $\rightarrow \infty$)	18.6 ± 0.39	$(22.6 \pm 1.41)^a$	0.82 ± 0.07	1.52 ± 0.021	10.95	0.50		0.48

^a Data measured using the Lee–Yang approach from ref. 6. ^b Average viscosity (μ) for the reaction solutions of various CRL–AuNP conjugate systems.

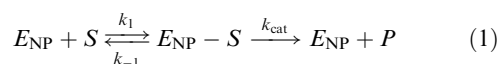
completely, R remained constant over time (*i.e.*, no aggregation). In contrast, significant decreases in R occurred (*i.e.*, aggregation) when the enzyme content was insufficient. We define the coverage as the ratio $(R - R_{\text{min}})/(R_{\text{max}} - R_{\text{min}})$, where R_{max} and R_{min} are the ratios (A_{peak}/A_{620}) in the presence of sufficient enzyme to provide colloidal stability and in the absence of enzyme (*i.e.*, fully aggregated), respectively. Fig. S6 (in ESI†) reveals the quantitative relationship between the percentage coverage of the AuNPs of various sizes and the CRL concentration; the values of C_{p} are determined at 50% coverage.

For the preparation of CRL–AuNP conjugates, the sufficient concentration of CRL (10-fold C_{p} of each set of CRL–AuNP complexes) was mixed with the AuNP solution of various sizes to ensure colloidal stability. The functionalized conjugates were washed repeatedly using centrifugation to remove excess enzyme. To assure that all unbound CRL was removed from the colloidal suspensions, activity tests were performed on the supernatants from the centrifugation/washing procedure. Table S1 (in ESI III†) shows the drop in activity to zero as the conjugates are repeatedly cleaned. This procedure was repeated six times until no activity was measured to ensure the absence of free CRL in the systems. To detect the CRL loading on the AuNPs, KCN was used to oxidize and dissolve the AuNPs, thereby liberating the bound CRL from the surfaces of the conjugates. For AuNPs having mean sizes of 13.1, 25.2, 37.5, 50.8, and 69.6 nm, the enzyme concentrations were 104.3 ± 3.2 , 61.7 ± 0.8 , 16.5 ± 0.6 , 11.0 ± 0.1 , and 6.8 ± 0.1 nM, respectively. These values were reported for the activity assays of various CRL–AuNP conjugate systems.

Using UV–Vis spectrophotometry, we detected the activities of the CRL–AuNP conjugates by measuring the absorbance of *p*-nitrophenol (*p*NP), a hydrolysis product from *p*NPP, at 405 nm. In Fig. S9 (see ESI V†), we observed that the initial release of *p*NP was proportional to the reaction time of various CRL–AuNP conjugated systems; in the inset of relative activity, there was a significant increase in the catalytic activity in the system featuring the smaller NPs, revealing that the size of the AuNPs was an important factor for the modulation of enzyme activity.

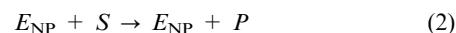
In the enzymatic kinetics experiment, Michaelis–Menten plots for the hydrolysis of *p*NPP (5.55–133.33 μM) catalyzed by the CRL–AuNP conjugates incorporating AuNPs of various average sizes are displayed in Fig. S10 (see ESI VI†); the experiment-measured catalytic parameters are listed in Table 1. Although the turnover numbers k_{cat} for the various-sized AuNPs were similar, the Michaelis constants K_{m} for the

smaller AuNPs had lower values. In previous studies,⁶ we found that the kinetics of the enzyme immobilized on one side of a planar surface could be effectively modeled and measured; in Table 1, when varying the AuNPs' dimensions, the values of K_{m} displayed an increasing trend in the presence of larger AuNP size, even under the extreme condition of AuNP size $\rightarrow \infty$. In simple terms, the rate constants for the individual steps are described in eqn (1):



An obtained lower value of K_{m} [$(k_{-1} + k_{\text{cat}})/k_1$] represented greater kinetic affinity between the enzyme and the substrate; *i.e.*, the conjugated system with the smaller AuNPs exhibited enhanced kinetic affinity, thereby improving the catalytic efficiency $k_{\text{cat}}/K_{\text{m}}$.

To further correlate the NP dimensions (size effect) to the catalytic efficiency ($k_{\text{cat}}/K_{\text{m}}$) of the conjugated enzyme, we developed a shielding model based on diffusion–collision theory (a detailed derivation is given in the ESI†, p. 14, theoretical considerations). We made the following assumptions: (i) the NPs, enzymes, and substrate molecules behaved as “rigid balls” (*cf.* Fig. 1); (ii) the intrinsic properties of the enzymes conjugated onto the differently sized NPs were similar; and (iii) the orientation of the active site of the enzyme–NP conjugates was random. Without considering multistep reactions, the catalytic reaction of substrate S with the conjugated enzyme E_{NP} can be approximated as the bimolecular reaction (Fig. 1(a)) in eqn (2).



The reaction rate ν ($\mu\text{M s}^{-1}$) can be expressed as the product of the bimolecular rate constant $k_{\text{E-NP}}^{\text{coll}}$ ($\mu\text{M}^{-1}\text{s}^{-1}$) and the concentrations of the enzyme (C_{E}) and substrate (C_{S}), as in eqn (3).

$$\nu = k_{\text{E-NP}}^{\text{coll}} C_{\text{E}} C_{\text{S}} \quad (3)$$

Relative to the free enzyme in solution, the E_{NP} provided additional steric hindrance for the binding of the substrate to the enzyme. We defined the shielding factor η as the solid-angle ratio of the enzyme surface exposed to substrate bombardment; the open solid-angle fraction Ω was displayed in Fig. 1(c) with respect to the full solid angle 4π . Furthermore, combining diffusion–collision theory, the shielding effect (on the modulation of the probability of bombardment) and

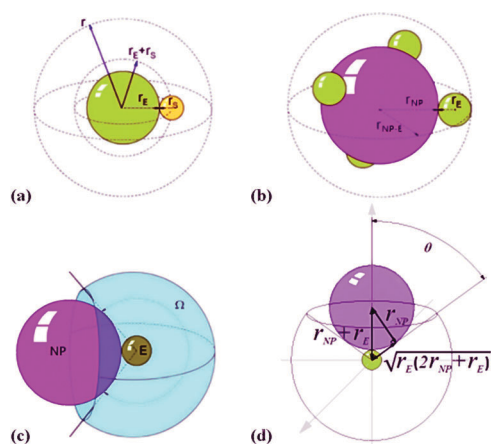


Fig. 1 Geometric relationships between the substrate S , the enzyme E and the nanoparticle NP . (a) If the distance between the S and E was less than the sum of the radii of two bounding spheres, $r_E + r_S$, then a collision event occurred. (b) Concerning diffusion effects in a fluid, the effective radius of the enzyme–NP conjugate should increase to $r_{NP} + 2r_E$. (c) The solid-angle fraction Ω exposed for collisions between the substrate and the enzyme. (d) Geometric relationships of the respective radii.

the Stokes–Einstein equation (the relationship between the diffusion coefficient and radius), we derived eqn (4)–(6) to model the size effect:

$$k_{E-NP}^{\text{coll}} = Z \cdot p \cdot \eta \cdot e^{-\frac{E_{\text{act}}}{RT}} = k_{\text{max}}^{\text{eff}} \cdot \eta \cdot e^{-\frac{E_{\text{act}}}{RT}} \quad (4)$$

$$k_{\text{max}}^{\text{eff}} = \frac{RT}{1500\mu} \left(\frac{1}{r_{NP} + 2r_E} + \frac{1}{r_S} \right) (r_E + r_S) \quad (5)$$

$$\eta = \frac{\Omega}{4\pi} = \frac{1}{2} \left[1 + \frac{\sqrt{r_E(2r_{NP} + r_E)}}{r_{NP} + r_E} \right] \quad (6)$$

where Z ($\mu\text{M}^{-1} \text{s}^{-1}$) is the frequency of collisions; p the fraction of substrates that are in the correct orientation; E_{act} the activation energy; R the gas constant; and T the absolute temperature; μ is the viscosity of the reaction mixture; $k_{\text{max}}^{\text{eff}}$ ($\mu\text{M}^{-1} \text{s}^{-1}$) the maximum frequency of effective collisions for the system (*i.e.*, $\eta \rightarrow 1$ and $E_{\text{act}} = 0$); Ω the solid-angle fraction of the enzyme surface open to substrates; and r_{NP} , r_E , and r_S are the radii of the NP, enzyme, and substrate, respectively.

Substituting the viscosity, absolute temperature, and radii ($r_E = 5.17$ nm; $r_S = 0.58$ nm; evaluated in the ESI†, Sections VII and VIII, respectively) into eqn (4)–(6) gave the bimolecular rate constants k_{E-NP}^{coll} listed in Table 1. For the AuNPs having average diameters in the range 13.1–69.6 nm, the theoretical rate constants k_{E-NP}^{coll} and the specificity constant k_{cat}/K_m (in Table 1) followed identical trends. In this model, when considering the extreme condition of $r_{NP} \rightarrow \infty$, the theoretical rate constant became 39.3% (0.48/1.22) of that for the system having a mean AuNP size of 13.1 nm. In comparison with the measured catalytic efficiency in Table 1, the enzyme immobilized onto a planar surface was 43.4% (0.82/1.89) of that of the system featuring AuNPs having a mean size of 13.1 nm. This percentage change was fairly consistent with the theoretical value. The enhanced activity by size-effect would theoretically converge to a finite maximum value when the AuNP size

approached zero. Within the model of classical enzymatic kinetics, the shielding factor mainly affected the rate constant k_1 , not k_{-1} or k_{cat} in eqn (1); that is, the steric hindrance affected only the binding path of the substrates, and not the desorption of the complex $E_{NP} \cdot S$. Table 1 revealed that the values of k_{cat} were almost independent of the AuNP size, whereas the values of K_m correlated strongly with it. Thus, this size-effect model had physical meaning and reasonably explained the kinetic response of this enzyme–NP conjugate system.

In summary, we had performed a series of experiments to systematically analyze the modulated NP size-dependent enzymatic activities of CRL–AuNP conjugates, and had developed a shielding model to explain the correlation between the size effects and the kinetic responses. A simple and efficient method for the preparation of this functional conjugates, with colloidal stability, under retention of enzymatic activity had been reported. The association of CRL with the AuNPs did not influence the values of k_{cat} , but the smaller AuNPs promoted the catalytic efficiency of CRL by increasing its kinetic affinity (*i.e.*, lower K_m values) toward the substrate pNPP. In this study, we found that the sizes of these conjugates acted as a controllable and efficient factor for modulating the activity of the enzyme. We believed that as the integrative field of nano-biotechnology evolves, such studies of the fundamental interactions of nanostructures with biological systems will become, by necessity, more common.

Notes and references

- 1 N. C. Price and L. Stevens, in *Fundamentals of Enzymology: The Cell and Molecular Biology of Catalytic Proteins*, Oxford University Press, New York, 1999, 3rd edn, pp. 347–355.
- 2 C. A. Mirkin, R. L. Letsinger, R. C. Mucic and J. J. Storhoff, *Nature*, 1996, **382**, 607; H. E. Schoemaker, D. Mink and M. G. Wubbolts, *Science*, 2003, **299**, 1694; C.-C. Wu, F.-H. Ko, Y.-S. Yang, D.-L. Hsia, B.-S. Lee and T.-S. Su, *Biosens. Bioelectron.*, 2009, **25**, 820.
- 3 A. Verma and V. M. Rotello, *Chem. Commun.*, 2005, 303; J. L. Brennan, N. S. Hatzakis, T. R. Tshikhudo, N. Dirvianskyte, V. Razumas, S. Patkar, J. Vind, A. Svendsen, R. J. M. Nolte, A. E. Rowan and M. Brust, *Bioconjugate Chem.*, 2006, **17**, 1373; S. Maiti, D. Das, A. Shome and P. K. Das, *Chem.–Eur. J.*, 2010, **16**, 1941.
- 4 Q. G. Wang, Z. M. Yang, L. Wang, M. L. Ma and B. Xu, *Chem. Commun.*, 2007, 1032; Q. G. Wang, Z. M. Yang, Y. Gao, W. W. Ge, L. Wang and B. Xu, *Soft Matter*, 2008, **4**, 550.
- 5 R. Haag and F. Kratz, *Angew. Chem., Int. Ed.*, 2006, **45**, 1198.
- 6 C.-C. Lee, H.-P. Chiang, K.-L. Li, F.-H. Ko, C.-Y. Su and Y.-S. Yang, *Anal. Chem.*, 2009, **81**, 2737.
- 7 M. De, P. S. Ghosh and V. M. Rotello, *Adv. Mater.*, 2008, **20**, 4225.
- 8 H. F. Jia, G. Y. Zhu and P. Wang, *Biotechnol. Bioeng.*, 2003, **84**, 406.
- 9 M. Brust, J. Fink, D. Bethell, D. J. Schiffrin and C. J. Kiely, *J. Chem. Soc., Chem. Commun.*, 1995, 1655; C. M. Niemeyer, *Angew. Chem., Int. Ed.*, 2001, **40**, 4128; R. Baron, B. Willner and I. Willner, *Chem. Commun.*, 2007, 323; U. H. F. Bunz and V. M. Rotello, *Angew. Chem., Int. Ed.*, 2010, **49**, 3268.
- 10 C.-S. Wu, C.-T. Wu, Y.-S. Yang and F.-H. Ko, *Chem. Commun.*, 2008, 5327.
- 11 G. Krauss, in *Biochemistry of Signal Transduction and Regulation*, Wiley-VCH, Weinheim, 2nd edn, 2001.
- 12 P. Free, C. P. Shaw and R. Levy, *Chem. Commun.*, 2009, 5009.
- 13 R. D. Schmid and R. Verger, *Angew. Chem., Int. Ed.*, 1998, **37**, 1608.